NMR IN BIOMEDICINE, VOL. **10**, 197–203 (1997)

A Hypercapnia-Based Normalization Method for Improved Spatial Localization of Human Brain Activation with fMRI

Peter A. Bandettini[1]* and Eric C. Wong[2]

[1] Medical College of Wisconsin, Biophysics Research Institute, Milwaukee, WI 53226, USA
[2] University of California—San Diego, Departments of Radiology and Psychology, San Diego, CA 92103, USA

An issue in blood oxygenation level dependent contrast-based functional MRI is the accurate interpretation of the activation-induced signal changes. Hemodynamic factors *other than* activation-induced changes in blood oxygenation are known to contribute to the signal change magnitudes and dynamics, and therefore need to be accounted for or removed. In this paper, a general method for removal of effects other than activation-induced blood oxygenation changes from fMRI brain activation maps by the use of hypercapnic stress normalization is introduced. First, the effects of resting blood volume distribution across voxels on activation-induced BOLD-based fMRI signal changes are shown to be significant. Second, the effects of hypercapnia and hypoxia on resting and activation-induced signal changes are demonstrated. These results suggest that global hemodynamic stresses may be useful for non-invasive mapping of blood volume. Third, the normalization technique is demonstrated.

NMR Biomed. **10**, 197–203 (1997) No. of Figures: 9 No. of Tables: 0 No. of References: 44

Keywords: deoxyhemoglobin; hypercapnia; fMRI; BOLD; hypoxia; brain mapping

Received 30 January 1997; accepted 18 March 1997

INTRODUCTION

The utility of functional magnetic resonance imaging (fMRI) as a brain mapping tool is directly related to the degree to which the relationship between MRI signal changes and underlying neuronal activation can be established. Two 'filters' separate direct observation of neuronal processes using fMRI. The first is the relationship between neuronal activation and hemodynamic changes, and the second is the relationship between hemodynamic changes and MRI signal changes.

During neuronal activation, measurable electromagnetic[1–4] and metabolic[1, 5–10] changes are produced. Through incompletely understood mechanisms[1, 11–18] these changes are accompanied by changes in blood flow,[11, 12, 15–23] volume,[11, 24–27] and oxygenation.[11, 26–30] It is not known whether these changes are constant across tasks and across regions in the brain, or exactly what mediates them.

In the past five years, progress has been made in the characterization of the relationship between activation-induced hemodynamic changes and fMRI signal changes. Perfusion and oxygenation changes in capillaries are closer in both space and time to neuronal activation than those arising from arteries or veins. While fMRI pulse sequences can be sensitized to specific populations of vessel sizes, blood flow velocities, and contrast mechanisms, T_2^*-weighted imaging using blood oxygenation level dependent (BOLD) contrast is most commonly used for fMRI because it has the highest functional contrast to noise ratio of any other fMRI sequence by about a factor of two to four. The drawback of T_2^*-weighted imaging is that the functional contrast includes, along with subtle capillary oxygenation changes, large vessel 'downstream' draining vein effects and, in the case of short *TR*-high flip angle sequences (short *TR* values are required for non-EPI fMRI sequences), large vessel 'upstream' arterial inflow effects. In fact, as will be demonstrated, the fMRI signal is strongly weighted by the blood volume in each voxel. Large vessels may cause voxels to have as high as 100% blood volume. These large vessel effects can be misleading unless identified and/or removed.

In this paper, a method for removal of large draining vein effects from brain activation maps by the use of a hypercapnic stress is introduced. First, the theory and rational behind using a hypercapnic stress to remove large downstream vein effects from brain activation maps is described. Second, the effects of hypercapnia and hypoxia on global T_2^*-weighted signal and on activation-induced signal changes are shown. Third, the normalization technique is demonstrated.

THEORY

A concern in BOLD contrast based fMRI is that factors other than blood oxygenation changes coincident with neuronal activation influence the magnitude of the activation induced signal changes. The effects of these other factors prevent quantification of neuronal activation, and comparison, using a single task, of activation magnitude across separate cortical regions. In addition, they may interfere with accurate assessment of the location and timing of neuronal activation. Biophysical models describing mechanisms of fMRI signal changes have been

* Correspondence to: Peter A. Bandettini; *email:* pab@post.its.mcw.edu

 CCC 0952–3480/97/040197–07 $17.50

published.[31–38] These models suggest that, in the case of BOLD contrast, the magnitude of the activation-induced signal change in each voxel is determined, among other factors, by vessel geometry, hematocrit, blood volume, and blood oxygenation changes. These models have indicated that resting state blood volume is one of the strongest determinants of the fMRI signal change magnitude, other than activation-induced oxygenation changes. For example, if two voxels in the brain have different blood volumes yet the vessels in each voxel undergo identical oxygenation changes with activation, the voxel with the higher blood volume will show a larger signal change. Simulations,[32] showing the effect of resting blood volume and oxygenation on transverse relaxation rate change, (Fig. 26 of Ref. 32) were used for illustrative purposes in this paper. This particular simulation, performed using a deterministic method to model spin diffusion effects,[39] assumed an average vein radius of 10 μm, a susceptibility difference, $\Delta\chi$, between fully oxygenated red blood cells and fully deoxygenated red blood cells, of $0{\cdot}18\times10^{-6}$ *cgs*, a random orientation of freely permeable vessels, a spin diffusion coefficient of 1 μm^2/ms, and a hematocrit of 42. A second-order polynomial fit to the simulated data was performed. Given that ΔR_2^* (s^{-1}) is the change in relaxation rate ($\Delta R_2^* = 1/T_2^* = -\ln(S'/S)/TE$, where S' is the MRI signal during a state when the blood is not 100% oxygen saturated, S is the MRI signal during a state when blood is 100% oxygen saturated, and TE is the echo time) that occurs with changing the blood oxygenation from 100% saturated, the relationship between ΔR_2^* and blood oxygenation and blood volume was approximated to be:

$$\Delta R_2^* = bv(1.81 - 3.38(O_2) + 1.57*(O_2)^2), \qquad (1)$$

where bv is blood volume (100 = 100% blood volume), and O_2 is fractional oxygen saturation (1 = 100% saturated). An isocontour plot of ΔR_2^* as a function of fractional blood volume and oxygenation is shown in Fig. 1.

Considering that a TE of 40 ms is typically used in functional imaging experiments to maximize sensitivity to susceptibility changes, the fractional MRI signal change (Δ%MRI), given a change in R_2^*, is described by:

$$\Delta\%\text{MRI} = 100\times(e^{-(\Delta R_2^*0.04)} - 1). \qquad (2)$$

Considering a resting state, hemoglobin oxygenation saturation of 60%. The dependence of Δ%MRI on resting state fractional blood volume and activation-induced change in hemoglobin saturation can be expressed as:

$$\Delta\%\text{MRI} = 100(-1 + e^{-0.04(-0.3472bv + bv(1.81 - 3.38(0.6+O_2) + 1.57(0.6+O_2)^2))}). \qquad (3)$$

An isocontour plot of Δ%MRI (assuming a resting blood oxygenation of 60%) as a function of hemoglobin saturation change and resting state fractional blood volume is shown in Fig. 2. The plotted range in hemoglobin saturation change is from 0 (no change) to 0.15 (typical of the change in venous blood oxygenation that occurs with brain activation), and the plotted range in fractional blood volume is from 0 to 60% blood volume (a typical range of what occurs across MRI voxels in the brain). It is assumed that the primary source of blood volume variation is over space and not coincident with activation.

Note in Fig. 2, as an example, that if the blood volume increases from 5 to 20% (i.e. a voxel in cortex and a voxel containing a draining vein) the activation-induced fractional MRI signal change, given an oxygenation change of 0.15 (60% saturation to 75% saturation), changes from an activation-induced increase of 2.5% ($bv = 5\%$) to an activation-induced increase of 15% ($bv = 20\%$). The method by which the variable effects of these blood volume differences over space can be taken into account is shown below.

A simulated cross-sectional sample of voxels is shown in Fig. 3 for illustrative purposes. First, the origin of the oxygenation change that occurs during brain activation is shown as the vertical bar in the center of the graph. This represents the region of cortex where neuronal firing and arteriole dilatation takes place. The activation-induced oxygenation change is shown to drop off exponentially over space. The horizontal dotted line represents a global increase in oxygenation that is induced by hypercapnia[40–42] or acetazolamide.[43]

Figure 3(b) shows the hypothetical distribution of blood volume over space across the same cross section. Vein blood volumes are shown by the solid line and capillary blood volumes are shown by the dotted line. Capillary blood volume is in the range of 2 to 5% and is somewhat homogeneously distributed over space. The blood volume

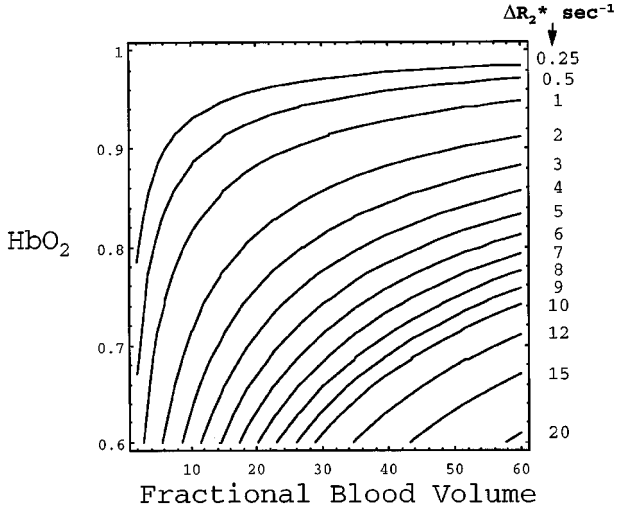

Figure 1. Isocontour plot, based on the relationship derived from simulations[32], of ΔR_2^* as a function of fractional blood volume and oxygenation. This plot demonstrates that resting state blood volume in each voxel is an extremely strong determinant of ΔR_2^* with a change in oxygenation.

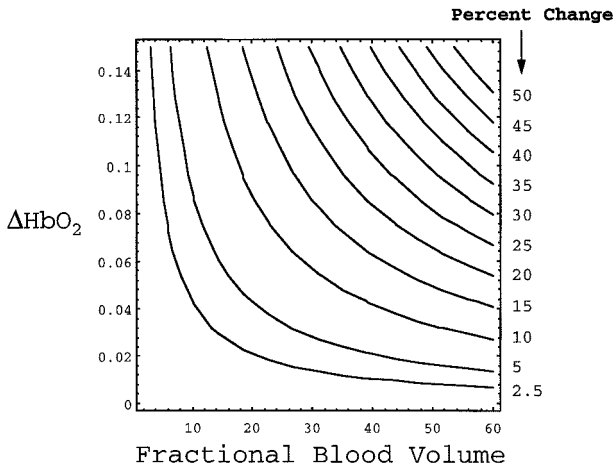

Figure 2. Isocontour plot of the fractional MRI signal change (assuming a resting blood oxygenation of 60%) as a function of hemoglobin saturation change and resting state fractional blood volume. The range of hemoglobin saturation change is from 0 (no change) to 0.15 (typical of the change in venous blood oxygenation that occurs with brain activation), and the plotted range in fractional blood volume is from 0 to 60% blood volume.

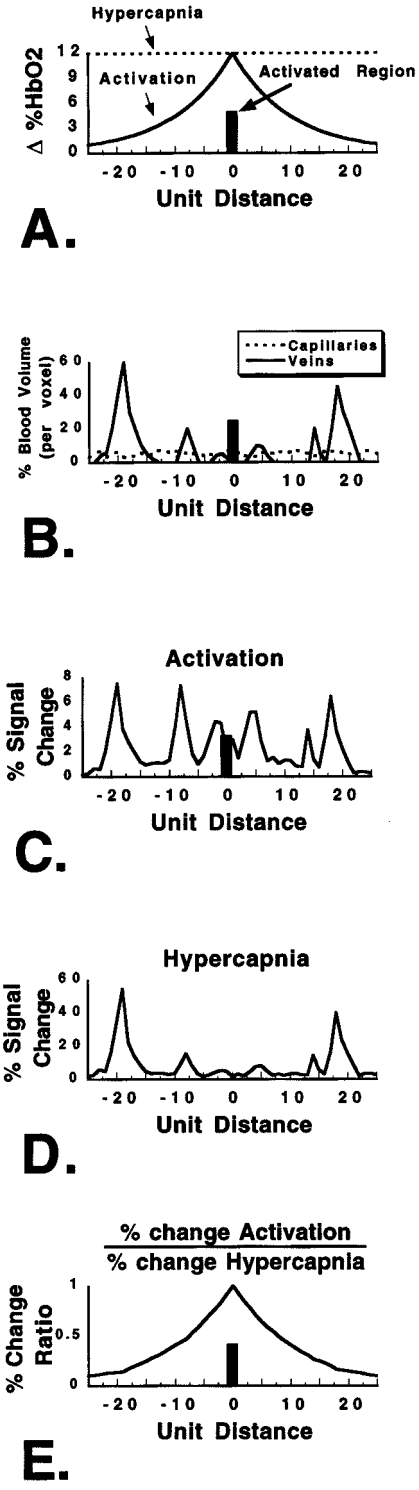

Figure 3. Hypothetical cross-sectional samples of voxels from an image of the brain. (a) Normalized in oxygenation that occurs in the brain as a result of brain activation (solid line) and hypercapnia (dotted line). The source of brain activation is indicated as the black bar at center. Hypoxia creates a global increase in oxygenation, (b) Typical blood volume distribution. Vein blood volumes (more heterogeneously distributed) are shown by the solid line and capillary blood volumes are shown by the dotted line, (c) Calculated, based on eq. (3), fractional signal change with brain activation, (d) Calculated fractional signal change with hypercapnia, (e) Fractional signal change with activation divided by fractional signal change with hypercapnia. This calculation removes the effect of blood volume heterogeneity across voxels and allows accurate localization of the voxels with the greatest activation-induced oxygenation changes.

from large vessels is more heterogeneous since the scale of the vessel size and spacing is similar to the voxel size. In a typical MRI image, the blood volume per voxel can vary from 5 to 60%.

Figure 3(c) and (d) are the calculated fractional signal changes over space with activation and with hypercapnia, based on the relationship in Equation 3, which takes into consideration the blood volume (from Fig. 3(b)), and the relative oxygenation change (from Fig. 3(a)). As can be seen, the magnitude of the signal change is highly weighted by the blood volume in each voxel. Note that the magnitude of the signal change in Fig. 3(c) is not reflective of the largest oxygenation change but is instead weighted by large vessel effects. This is the classic 'large vessel effect' in BOLD contrast fMRI.

Assuming that hypercapnia and neuronal activation cause similar hemodynamic events, one which is a global increase in oxygenation and the other which is a local increase in oxygenation, then the division of a 'fractional change during brain activation' image by a 'fractional change during hypercapnia' image would give a ratio map that is normalized to the signal change accompanying global vasodilatation, and would then have these 'large vessel effects' removed. Figure 3(e) illustrates this concept. In Fig. 3(e), the plot in Fig. 3(c) is divided by the plot in Fig. 3(d). The resulting plot is very similar to the plot in Fig. 3(a), which shows the actual activation-induced oxygenation change over space. The source of vasodilatation is accurately determined. If the assumption that blood volume in each voxel is the hemodynamic factor that most strongly determines BOLD-based fMRI signal changes, given an oxygenation change, then the fractional signal change maps produced by a hypercapnic stress can be used to completely remove 'large vessel effects' in fMRI. This method is demonstrated below.

EXPERIMENTAL

Single shot saggital gradient-echo echo-planar images containing the motor cortex were obtained using a GE 1.5 T Signa scanner, a 30.5 cm i.d. three-axis local gradient coil, and a whole-brain endcapped quadrature transmit/receive birdcage RF coil. Voxel volume $= 3.75 \times 3.75 \times 5\ \text{mm}^3$, $TE = 40$ ms, and $TR = 2$ s. Seven time course series were obtained. In each time course series, 120 sequential images were collected. Each time course series was separated by a 5 min rest period.

The trials performed were as follows. Trials 1 and 2: Hypoxia (breathing of 12% O_2) for a duration of 3 min, starting after 30 s of breathing room air. No finger movement was performed. Trials 3 and 4: Hypercapnia (breathing of 5% CO_2) for a duration of 3 min, starting after 30 s of breathing room air. No finger movement was performed. Trial 5: Cyclic bilateral finger movement (10 s 'on' and 20 s 'off') during the entire time course, while breathing room air. Trial 6: Cyclic bilateral finger movement (entire time series) combined with hypoxia (starting after 30 s). Trial 7: Cyclic bilateral finger movement combined with hypercapnia (starting after 30 s).

From Trial 5, the activated motor cortex region was obtained using correlation analysis.[44] All subsequent voxel-wise analysis was performed on those voxels that demonstrated a correlation coefficient, in Trial 5, above 0.5 with a reference boxcar function representing the motor

cortex task timing. Comparisons were made of the magnitudes of the stress (hypercapnia or hypoxia)-induced and the activation-induced fractional signal changes either on a voxel-wise basis or on a region of interest (averaging over space) basis.

RESULTS

Figure 4(a) shows an anatomical echo-planar image of the slice chosen. Fig. 4(b) shows a brain activation image obtained by calculation of the dot product of a reference function representing the expected activation-induced response with the time course from Trial 5. Figure 4(c) and (d) show images obtained by subtraction of the average of image numbers 10–20 (baseline) from the average of image numbers 40–120 in time courses of Trials 1 and 2 (hypoxia), respectively. Figure 4(e) and (f) show images obtained by subtraction of the average of image numbers 10–20 (baseline) from the average of image numbers 40–120 in time courses of Trials 3 and 4 (hypercapnia), respectively. The results are highly reproducible and the patterns of signal change during hypercapnia and hypoxia are similar in magnitude yet opposite in sign. Regions of highest blood volume (sinuses) appear to show the largest signal changes with the global stresses *and* during finger movement.

From a region in motor cortex, the average signal changes were: Trial 1, $-8.1 \pm 1.0\%$; Trial 2, $-8.8 \pm 1.2\%$; Trial 3, $10.0 \pm 1.5\%$; Trial 4, $7.3 \pm 1.4\%$; Trial 5, $2.6 \pm 0.3\%$.

Time course plots from a single region of interest, from Trials 1 through 4 are shown in Fig. 5. During hypercapnia, a signal increase is observed, demonstrating that an increase in flow without an increase in the oxygen extraction rate caused an overall increase in oxygenation. During hypoxia, the baseline signal decreased, suggesting that the arterial oxygenation decreased without significant compensatory vasodilatation, causing the blood oxygenation to decrease. This study helps to further establish the sensitivity of this sequence to oxygenation changes and not to flow changes, since hypoxia is not known to cause decreases in flow.

Time course plots corresponding to Trials 5 through 7 are shown in Fig. 6. The amplitude of the activation-induced signal change was significantly damped during hypercapnia. During hypoxia, the amplitude of the activation-induced signal change was only slightly damped. Because hypoxia does not cause significant increases in flow, it does not damp activation-induced signal changes.

A voxel-wise comparison was made between brain activation-induced signal changes (while breathing room air) and signal changes caused by hypoxia and hypercapnia (during no finger movement). Figure 7 is a voxel-wise comparison of signal change during finger movement with

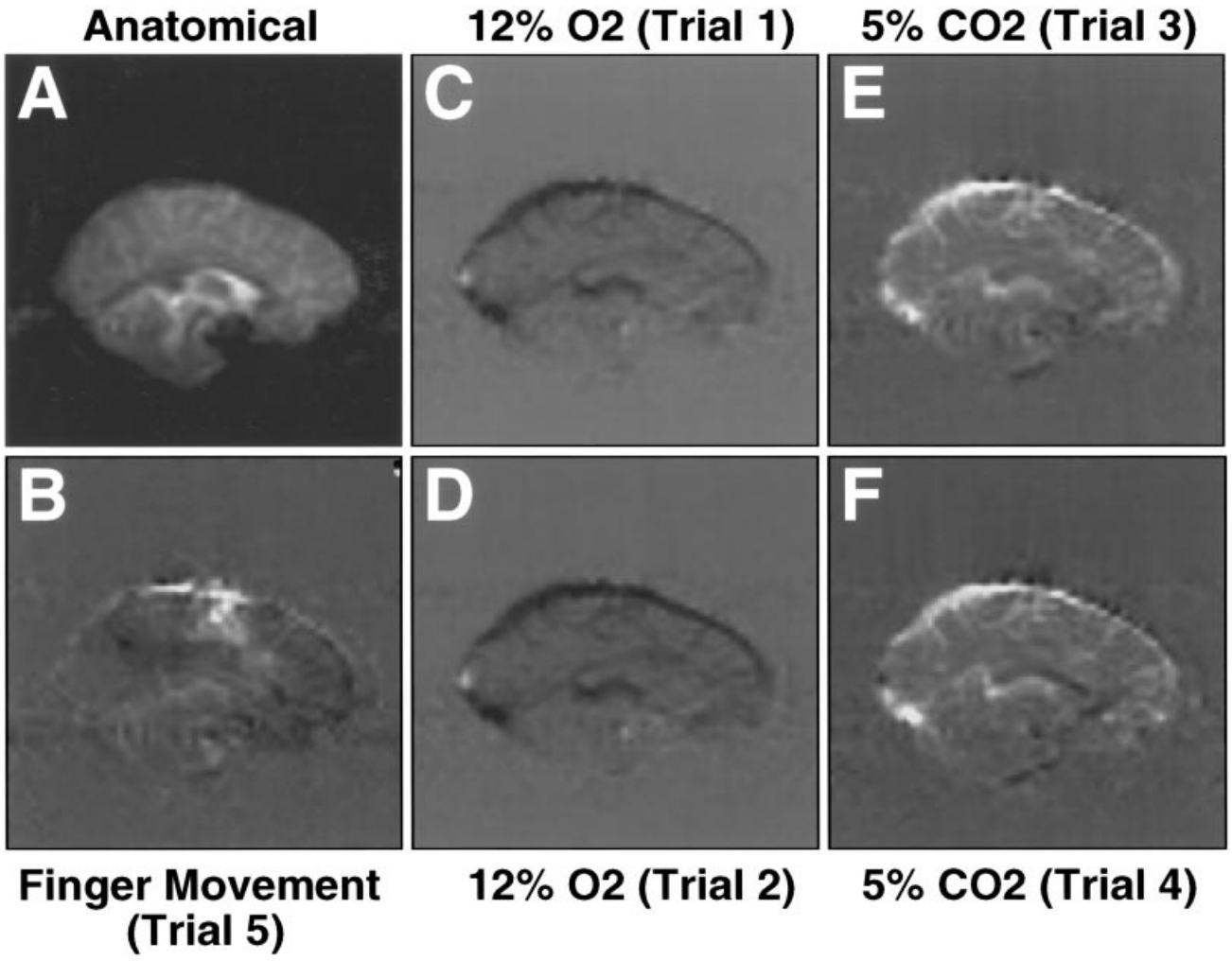

Figure 4. (a) Anatomical echo-planar image, (b) Brain activation image (finger movement) from Trial 5, (c) and (d) Average stress (hypoxia: image numbers 40–120)—average baseline (image numbers 10–20) from Trials 1 and 2, (e) and (f) Average stress (hypercapnia: image numbers 10–120)—average baseline (image numbers 10–20) from Trials 3 and 4.

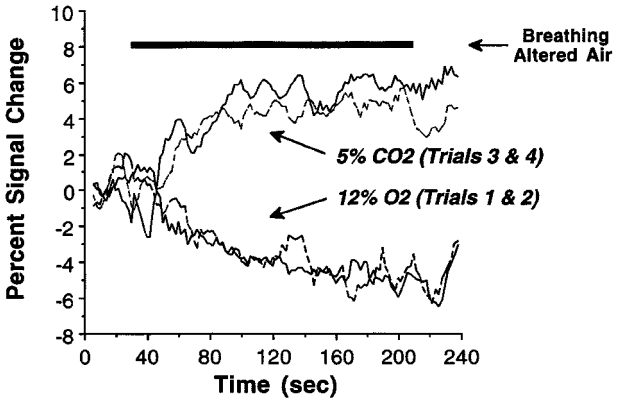

Figure 5. MRI signal from a 15 voxel region in motor cortex during two Trials (Trials 1 and 2) of hypoxia (12% O_2) and two Trials (Trials 3 and 4) of hypercapnia (5% CO_2).

the signal changes during hypoxia (average of 1 and 2) or hypercapnia (average of 3 and 4). The changes appear to be proportional to one another. The voxel with the largest signal change with activation also corresponds to the voxel with the largest signal change during hypercapnia or hypoxia.

Figure 8 is a voxel-wise plot of 'percent change during

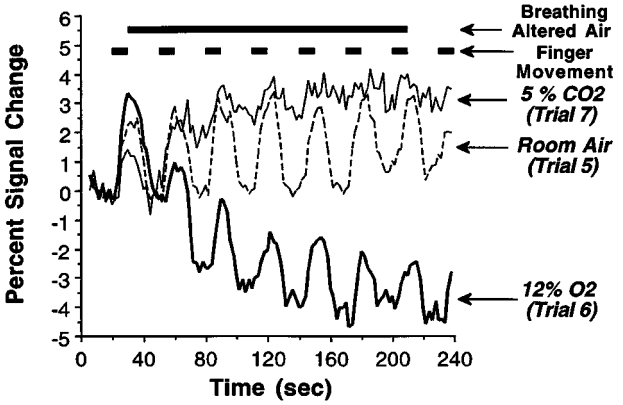

Figure 6. MRI signal from the same 15 voxel region as in Fig. 5 during combinations of cyclic on-off finger movement and breathing of room air (Trial 5), finger movement and hypoxia (Trial 6), finger movement and hypercapnia (Trial 7).

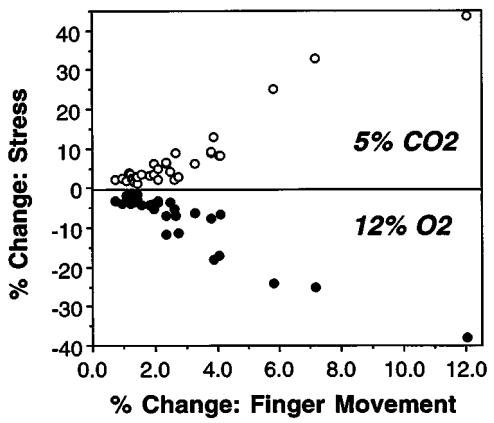

Figure 7. Voxel-wise scatter plot comparison (32 voxels) of signal change during finger movement with the signal changes during hypoxia (average of Trials 1 and 2) or hypercapnia (average of Trials 3 and 4). The changes appear to be proportional to one another, suggesting that factors other than blood oxygenation changes, (specifically resting state blood volume differences over space) contribute significantly to activation-induced BOLD signal change magnitude.

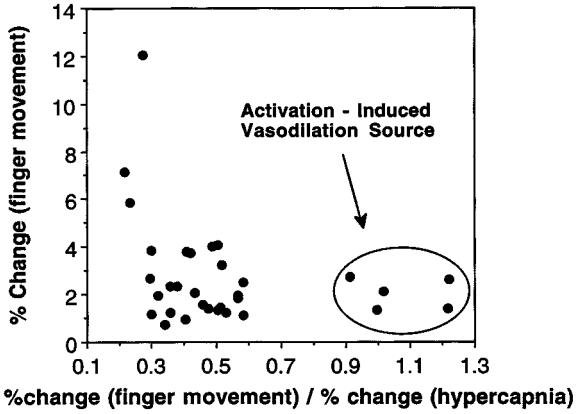

Figure 8. Voxel-wise plot of 'percent change during finger movement', vs 'percent change during finger movement + percent change during hypercapnia' from the same voxels as shown in Fig. 7. Several voxels have a ratio ≈ 1. It is hypothesized that, in these voxels, the strongest activation-induced vasodilatation has taken place.

finger movement' vs 'percent change during finger movement + percent change during hypercapnia' from the 32 voxels in the region showing activation. Several voxels have a ratio of approximately 1. It is hypothesized that, in these voxels, the strongest activation-induced vasodilatation has taken place, as explained in Fig. 3. Note that the largest changes prior to normalization (*y*-axis), have nearly the smallest ratios (*x*-axis), indicating that the actual activation-induced oxygenation change in these voxels may have been minimal (downstream), but a large blood volume in these particular voxels has amplified the percent signal change. The relative signal change magnitudes before and after division of the activation-induced percent signal change map by the hypercapnia percent signal change map, (here Trial 4 is used), are shown in Fig. 9 The region of highest signal change, after division by a 'percent change during hypercapnia' mask, has moved from the sagittal sinus to a region apparently in cortex.

CONCLUSIONS

Within the region that demonstrated changes during activation, the spatial pattern of signal change caused by finger movement was similar to the pattern created by the global stresses. This suggests, along with prior simulation studies, that the primary cause for spatial variation in signal change during activation is spatial heterogeneity in blood volume, and that the small gradient in blood oxygenation that extends away from the activation-induced source of vasodilatation only secondarily contributes to relative signal change magnitudes. Division of activation-induced percent change maps by hypercapnia-induced percent change maps successfully normalized the signal changes to differences in vessel architecture, leaving behind, as the highest signal intensity region, the area of activation-induced vasodilatation. This method may be necessary to increase functional resolution of fMRI and, in the future, may be useful in quantification of activation-induced flow changes, assuming the ability to quantify global hypercapnia-induced flow changes.

Several other observations may be drawn from this study. Hypercapnia increased the overall signal intensity, and damped activation-induced signal changes, demonstrating a

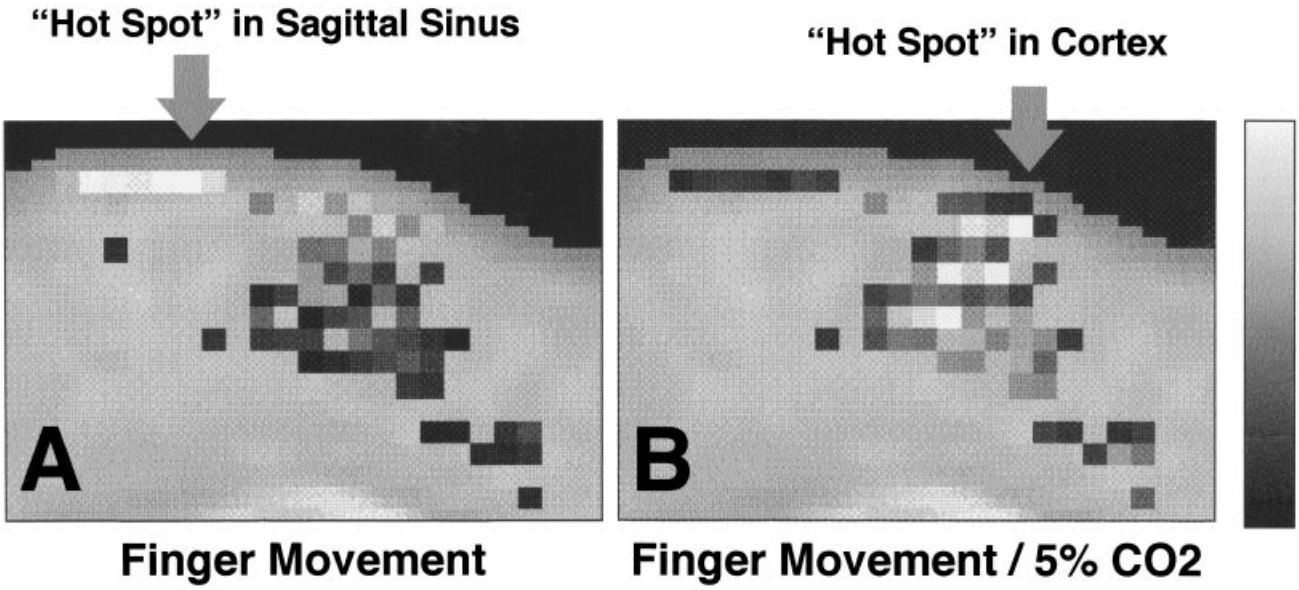

Figure 9. The relative signal change magnitudes: (a) before and (b) after division of the activation-induced percent signal change map by the hypercapnia percent signal change map, (here Trial 4 is used), are shown. The region of highest signal change, after division by a 'percent change during hypercapnia' mask, has moved from the sagittal sinus to a region apparently in cortex.

competitive, and possibly identical, signal change mechanism as that caused by neuronal activation. Hypoxia decreased overall signal intensity but did not as strongly damp the activation-induced signal changes. The lack of competition with activation-induced signal changes agrees with the understanding that hypoxia does not cause significant vasodilatation.

As simulated and demonstrated, the BOLD contrast-based signal changes are strongly weighted by blood volume in each voxel. If it is assumed that the oxygenation increase with hypercapnia is constant across the brain, then, because of this strong volume weighting of the fMRI signal change, the technique of administering a hypercapnic stress may also be useful for noninvasive mapping of cerebral blood volume.

Acknowledgements

The authors would like to express their gratitude to Dr Bert Forster, Dr Elizabeth Aaron, and Timothy Lowry from the department of Physiology at Medical College of Wisconsin. Thanks also to Lloyd Estkowski for his expert technical assistance.

REFERENCES

1. Roland, P. E. *Brain Activation.* Wiley, New York (1993).
2. Krnjevic, K. Coupling of neuronal metabolism and electrical activity. In *Brain Work*, ed. by D. H. Ingvar and N. A. Lassen, pp. 65. Munksgaard, Copenhagen (1975).
3. Hillyard S. G. and Picton, T. W. Electrophysiology of cognition. In *Handbook of Physiology, Section 1: Neurophysiology*, pp. 519. American Physiological Society, New York (1987).
4. Hari, R. On brain's magnetic responses to sensory stimuli. *J. Clinical Neurophysiol.* **8**, 157–169 (1991).
5. Prichard, J., Rothman, D., Novotny, E., Petroff, O., Kuwabara, T., Avison, M., Howsman, A., Hanstock, C. and Shulman, R. Lactate rise detected by ^{1}H NMR in human visual cortex during physiologic stimulation. *Proc. Natl Acad. Sci. USA* **88**, 5829–5831 (1991).
6. Merboldt, K.-D., Bruhn, H., Hanicke, W., Michaelis, T. and Frahm, J. Decrease of glucose in the human visual cortex during photic stimulation. *Magn. Reson. Med.* **25**, 187–194 (1992).
7. Fox, P. T., Raichle, M. E., Mintun, M. A. and Dence, C. Nonoxidative glucose consumption during focal physiologic neural activity. *Science* **241**, 462–464 (1988).
8. Phelps, M. E., Kuhl, D. E. and Mazziotta, J. C. Metabolic mapping of the brain's response to visual stimulation: studies in humans. *Science* **211**, 1445–1448 (1981).
9. Mazziotta, J. C. and Phelps, M. E. Human neuropsychological imaging studies of local brain metabolism: strategies and results. In *Brain Imaging and Brain Function*, ed. by L. Sokoloff, p. 121. Raven Press, New York (1985).
10. Haxby, J. L., Grady, C. L., Ungerleider, L. G. and Horowitz, B. Mapping the functional neuroanatomy of the intact human brain with brain work imaging. *Neuropsychologia* **29**, 539–555 (1991).
11. Villringer, A. and Dirnagle, U. Coupling of brain activity and cerebral blood flow: basis of functional neuroimaging. *Cereb. Brain Metab. Rev.* **7**, 240–276 (1995).
12. Gotoh, F. and Tanaka, K. Regulation of cerebral blood flow. In *Handbook of Clinical Neurology*, ed. by P. J. Vinkin, G. W. Bruyn and H. L. Klawans, p. 47. Elsevier, New York (1987).
13. Kushinsky, W. Coupling between functional activity, metabolism, and blood flow in the brain: state of the art. *Microcirculation,* **2**, 357–378 (1982–1983).
14. Busija, D. W. and Heistad, D. D. *Factors Involved in the Physiological Regulation of the Cerebral Circulation.* Springer, Berlin (1984).
15. Lou, H. C., Edvinsson, L. and MacKenzie, E. T. The concept of coupling blood flow to brain function: revision required? *Ann. Neurol.* **22**, 289–297 (1987).
16. Kuschinsky, W. Physiology of cerebral blood flow and metabolism. *Arzneimittel-Forschung* **41**, 284–288 (1991).
17. Moskalenko, Y. E., Weinstein, G. B., Demchenko, I. T., Kislyakov, Y. Y. and Krivchenko, A. I. *Biophysical Aspects of Cerebral Circulation.* Pergamon Press, Oxford (1980).
18. Mchedlishvili, G. *Arterial Behavior and Blood Circulation in the Brain.* Plenum Press, New York (1986).
19. Estrada, C., Mengual, E. and Gonzalez, C. Local NADPH-diaphorase neurons innervate pial arteries and lie close or project to intracerebral blood vessels: a possible role for nitric oxide in the regulation of cerebral blood flow. *J. Cereb. Blood Flow Metab.* **13**, 978–984 (1993).
20. Dirnagl, U., Lindauer, U. and Villringer, A. Role of nitric oxide in the coupling of cerebral blood flow to neuronal activation

in rats. *Neurosci. Lett.* **149**, 43–46 (1993).
21. Iadecola, C. Regulation of cerebral microcirculation during neural activity: is nitric oxide the missing link? *TINS* **16**, 206–214 (1993).
22. Ingvar, D. H. Patterns of brain activity revealed by measurements of regional cerebral blood flow. In *Brain Work*, ed. by D. H. Ingvar and N. A. Lassen, p. 397. Munksgaard, Copenhagen (1975).
23. Colebatch, J. G., Deiber, M.-P., Passingham, R. E., Friston, K. J. and Frackowiack, R. S. J. Regional cerebral blood flow during voluntary arm and hand movements in human subjects. *J. Neurophysiol.* **65**, 1392–1401 (1991).
24. Sandman, C. A., O'Halloran, J. P. and Isenhart, R. Is there an evoked vascular response? *Science* **224**, 1355–1356 (1984).
25. Belliveau, J. W., Kennedy, D. N., McKinstry, R. C., Buchbinder, B. R., Weisskoff, R. M., Cohen, M. S., Vevea, J. M., Brady, T. J. and Rosen, B. R. Functional mapping of the human visual cortex by magnetic resonance imaging. *Science* **254**, 716–719 (1991).
26. Villringer, A., Planck, J., Hock, C., Scheinkofer, L. and Dirnagl, U. Near infrared spectroscopy (NIRS): a new tool to study hemodynamic changes during activation of brain function in human adults. *Neurosci. Lett.* **154**, 101–104 (1993).
27. Fox, P. T. and Raichle, M. E. Focal physiological uncoupling of cerebral blood flow and oxidative metabolism during somato-sensory stimulation in human subjects. *Proc. Natl Acad. Sci. USA* **83**, 1140–1144 (1986).
28. Frostig, R. D., Lieke, E. E., Ts'o, D. Y. and Grinvald, A. Cortical functional architecture and local coupling between neuronal activity and the microcirculation revealed by *in vivo* high-resolution optical imaging of intrinsic signals. *Proc. Natl Acad. Sci. USA* **87**, 6082–6086 (1990).
29. Grinvald, A., Frostig, R. D., Siegel, R. M. and Bratfeld, E. High-resolution optical imaging of functional brain architecture in the awake monkey. *Proc. Natl Acad. Sci. USA* **88**, 11559–11563 (1991).
30. Frostig, R. D. What does in vivo optical imaging tell us about the primary visual cortex in primates? In *Cerebral Cortex*, ed. by A. Peters and K. S. Rockland, vol. 10 (pp. 331). Plenum Press, New York (1994).
31. Ogawa, S., Menon, R. S., Tank, D. W., Kim, S.-G., Merkle, H., Ellerman, J. M. and Ugurbil, K. Functional brain mapping by blood oxygenation level-dependent contrast magnetic resonance imaging: a comparison of signal characteristics with a biophysical model. *Biophys. J.* **64**, 803–812 (1993).
32. Bandettini, P. A. and Wong, E. C. Effects of Biophysical and physiologic parameters on brain activation-induced R_2^* and R_2 changes: simulations using a deterministic diffusion model. *Int. J. Imag. Syst. Technol.* **6**, 134–152 (1995).
33. Kennan, R. P., Zhong, J. and Gore, J. C. Intravascular susceptibility contrast mechanisms in tissues. *Magn. Reson. Med.* **31**, 9–21 (1994).
34. Yablonsky, D. A. and Haacke, E. M. Theory of NMR signal behavior in magnetically inhomogenous tissues: the static dephasing regime. *Magn. Reson. Med.* **32**, 749–763 (1994).
35. Haacke, E. M., Lai, S., Yablonski, D. A. and Lin, W. *In vivo* validation of the BOLD mechanism: a review of signal changes in gradient echo functional MRI in the presence of flow. *Int. J. Imag. Syst. Technol.* **6** , 153–163 (1995).
36. Boxerman, J. L., Bandettini, P. A., Kwong, K. K., Baker, J. R., Davis, T. L., Rosen, B. R. and Weisskoff, R. M. The intravascular contribution to fMRI signal change: Monte Carlo modeling and diffusion-weighted studies *in vivo*. *Magn. Reson. Med.* **34**, 4–10 (1995).
37. Boxerman, J. L., Hamberg, L. M., Rosen, B. R. and Weisskoff, R. M. MR contrast due to intravascular magnetic susceptibility perturbations. *Magn. Reson. Med.* **34**, 555–566 (1995).
38. Weisskoff, R. M., Zuo, C. S., Boxerman, J. L. and Rosen, B. R. Microscopic susceptibility variation and transverse relaxation: theory and experiment. *Magn. Reson. Med.* **31**, 601–610 (1994).
39. Wong, E. C. and Bandettini, P. A. A deterministic method for computer modelling of diffusion effects in MRI with application to BOLD contrast imaging. *Proc., SMRM, 12th Annual Meeting*, New York (1993).
40. Jezzard, P., Heinmann, F., Taylor, J., Despres, D., Wen, H., Balaban, R. S. and Turner, R. Comparison of EPI gradient-echo contrast changes in cat brain caused by respiratory challenges with direct simultaneous evaluation of cerebral oxygenation via a cranial window. *NMR Biomed.* **7**, 35–44 (1994).
41. Rostrup, E., Larsson, H. B. W., Toft, P. B., Garde, K., Thomsen, C., Ring, P., Sondergaard, L. and Henricksen, O. Functional MRI of CO_2 induced increase in cerebral perfusion. *NMR Biomed.* **7**, 29–34 (1994).
42. Bandettini, P. A., Aaron, E. A., Wong, E. C., Lowry, T. F., Hinks, R. S., Hyde, J. S. and Forster, H. V. Hypercapnia and hypoxia in the human brain: effects on resting and activation-induced MRI signal. *Proc., SMR, 2nd Annual Meeting*, San Francisco (1994).
43. Kleinschmidt, A., Steinmetz, H., Sitzer, M., Merboldt, K. D. and Frahm, J. Magnetic resonance imaging of regional cerebral blood oxygenation changes under acetazolamide in carotid occlusive disease. *Stroke* **26**, 106–110 (1995).
44. Bandettini, P. A., Jesmanowicz, A., Wong, E. C. and Hyde, J. S. Processing strategies for time-course data sets in functional MRI of the human brain. *Magn. Reson. Med.* **30**, 161–173 (1993).

